RECENT PLANKTONIC FORAMINIFERA FROM DEEP-SEA SEDIMENTS FROM THE EASTERN EQUATORIAL PACIFIC: PROXIES OF THE EQUATORIAL FRONT IN THE LATE QUATERNARY

Jose Ignacio Martinez and Geovanny Bedoya

ABSTRACT

Planktonic foraminifera recovered from 25 deep-sea sediment samples (core-tops) from the eastern Equatorial Pacific were analyzed for their geographic distribution and possible environmental controls. Samples collected deeper than the carbonate lysocline (~2800 m) show significant signs of dissolution, - when compared to sediment-trap samples -, resulting in the increase of the solution-resistant species *Neogloboquadrina dutertrei*, *Neogloboquadrina pachyderma* and *Globorotalia cultrata* and the reduction of the solution-susceptible species *Globigerinita glutinata*, *Globigerinoides ruber* and *Globigerinoides sacculifer*. Three bioprovinces were recognized by cluster analysis: (1) bioprovince I that occurs on the Cocos Ridge where *G. cultrata* and *N. pachyderma* are dominant, (2) bioprovince II that occurs on the Carnegie Ridge where *N. dutertrei*, *N. pachyderma* and *Globorotalia inflata* are dominant, and (3) bioprovince III that occurs in the Panama Basin where *G. sacculifer* and *G. ruber* are dominant. Bioprovinces I and II reflect a shallow thermocline induced by upwelling, although AOU, NO_3 and PO_4 and SiO_2 are significantly higher in the latter region. Bioprovince III reflects a deep-mixed layer and low nutrient contents. Possible proxies of the Equatorial Front in the past are: (1) the Shannon diversity index, evenness and the number of species that show a latitudinal break at ~1.5ºS and, (2) the *G. cultrata* / *G. dutertrei* ratio that decreases southward.

KEY WORDS: Planktonic foraminifera, Eastern Equatorial Pacific, Panama Basin, Deep-sea sediments, Micropaleontology

RESUMEN

Foraminíferos planctónicos recuperados de muestras del tope de 25 núcleos de aguas profundas del Oceano Pacifico Oriental son analizados respecto a las variables ambientales que controlan su distribución geográfica. Las muestras colectadas por debajo de la lisoclina de carbonatos (~2800m) muestran señales considerables de disolucion, - con respecto a las muestras de trampas de sedimentos -, dando como resultado el incremento en especies resistentes a la disolucion como *Neogloboquadrina dutertrei*, *N. pachyderma* y *Globorotalia cultrata* y el decrecimiento en especies suceptibles a la disolución como *Globigerinita glutinata, Globigerinoides ruber* y *Globigerinoides sacculifer*. Se reconocen tres bioprovincias, por análisis Cluster, así: (1) bioprovincia I que ocurre sobre la Dorsal de Cocos donde *G. cultrata* y *N. pachyderma* son dominantes, (2) bioprovincia II que ocurre sobre la Dorsal de Carnegie Ridge donde *N. dutertrei*, *N. pachyderma* y *Globorotalia inflata* son dominantes, y (3) bioprovincia III que ocurre en la Cuenca de Panama donde *G. sacculifer* y *G. ruber* son dominantes. Las bioprovincias I y II reflejan una termoclina somera inducida por surgencia oceanica (upwelling), aunque AOU, NO_3, PO_4 y SiO_2 son mucho mayores en la segunda bioprovincia. La bioprovincia III refleja una capa de mezcla profunda y un contenido bajo de nutrientes en el agua. Como posibles indicadores ("proxies") de la posicion del Frente Ecuatorial en el pasado se sugieren: (1) el Indice de diversidad de Shannon, la equidad ("evenness") y el número de especies los cuales muestran un cambio latitudinal mayor a ~1.5ºS y, (2) la relación *G. cultrata* / *N. dutertrei* que decrece hacia el sur.

PALABRAS CLAVE: Foraminíferos planctónicos, Oceano Pacifico Oriental, Cuenca de Panamá Sedimentos profundos, Micropaleontología

INTRODUCTION

The Panama Basin is a critical region for the understanding of Global Climate Change because it receives a huge volume of fresh water derived from the atmospheric transfer of moisture by the Trade Winds from the Atlantic to the Pacific Ocean. This transfer of moisture regulates the inter-oceanic difference in sea-surface salinity which ultimately drives the global circulation of the ocean, i.e. the so called "conveyor belt" (e.g. Broecker and Denton, 1989). The Panama Basin is also bathed by the cool nutrient-rich Peru Current and the warm and less fertile Equatorial Counter Current that meet along the Equatorial Front (e.g. Wooster, 1969; Pak and Zaneveld, 1974). This oceanographic setting is episodically disrupted by El Niño phenomenon. In the past this pattern would have differed considerably at the scale of glacial and interglacial cycles. Furthermore, the huge volume of palynological information on land makes the Panama Basin an ideal region for ocean-continent paleoclimate correlations following the recommendations of the international scientific community. Finally, sea-surface temperature (SST) reconstructions based on planktonic foraminiferal assemblages on the equatorial Pacific for the last glacial maximum (e.g. CLIMAP, 1976; Anderson et al., 1989) have remained in conflict with palynological evidences for the past 20 years despite the use of new proxies of paleotemperature, e.g. Sr/Ca in corals and alkenones (Uk37) extracted from deep-sea sediments. Therefore, more up-to-date SST reconstructions for the Panama Basin are needed in order to solve the conflicting results. Recently, SST reconstructions based on radiolarians have shown that cooling south of the Equatorial Front was significantly larger than suggested by CLIMAP (1976) for the last glacial maximum (LGM), i.e. ~5ºC compared to <2ºC (Pisias and Mix, 1997). Precise SST reconstructions are critical for the building of reliable climate and paleoclimate models; the predictive character of these models is, therefore, strongly dependent on SST as a boundary condition.

Planktonic foraminifera are: (1) one of the most abundant Protista groups in the world ocean, (2) easily identifiable and, (3) have not evolved during the Late Quaternary. These characteristics make planktonic foraminifera an ideal proxy for the reconstruction of sea-surface environmental variables, e.g. temperature and salinity. However, the reconstruction of these environmental variables and the structure of the upper water column are highly dependent on a deep knowledge of the ecology of planktonic foraminifera in a region.

Planktonic foraminifera ecological and paleoecological studies in the Eastern Equatorial Pacific (EEP) include: (1) plankton-tow samples (e.g. Fairbanks et al., 1982; Thiede, 1983), (2) sediment trap moorings (e.g. Thunell et al., 1983; Thunell and Reynolds, 1984), and (3) down-core deep-sea sediments (e.g. Faul et al., 2000). None of these studies, however, have focused on the distribution of planktonic foraminifera at the sea floor, except for a localized study on the continental shelf in front of the Nariño Department (Cortes et al., 1990). On a different approach, other studies have considered the distribution of planktonic foraminifera on the entire Pacific basin, for the reconstruction of past sea-surface temperatures (e.g. Mix et al., 1999). Therefore, this paper aims to explore the ecological distribution of Recent planktonic foraminifera from a number of core-top samples widely distributed in the EEP region.

Even though planktonic foraminifera recovered from deep-sea sediments are excellent proxies of upper-water conditions (mainly SST and productivity), carbonate dissolution, dispersal and reworking of sediments might greatly blur the original sea-surface signal. For the Panama Basin foraminiferal dissolution begins at ~2800 m (Thunell et al., 1981), whereas significant sediment reworking and dispersal occur over the Cocos and Carnegie Ridges due to the action of deep-sea currents (e.g. Van Andel, 1973; Kowsmann, 1973; Lonsdale and Malfait, 1974; Yamashiro, 1975). Therefore, in order to understand the environmental variables that control the distribution of planktonic foraminifera, the effects of dissolution and reworking need to be assessed.

Physical Oceanography of the Eastern Equatorial Pacific (EEP)

The EEP is located in the eastern extreme of the equatorial current system in the Pacific Ocean (Fig. 1a). Surface currents in the region include the west-flowing North and South Equatorial Currents (NEC and SEC) and their corresponding, east-flowing countercurrents (NECC and SECC), plus the Peru, or Humbolt Current (e.g. Tomczak and Godfrey, 1994). Both, the NEC and SEC are driven by the Trade winds. Therefore, they are stronger in the winter of their respective hemisphere, i.e. the NEC transports 45 Sv (Sverdrup = 10^6 m^3s^{-1}) of water with a speed of 0.3 ms^{-1} in February; whereas the SEC transports 27 Sv with a speed of 0.6 ms^{-1} in August (e.g. Tomczak and Godfrey, 1994). In February the stronger influence of the northeast Trade winds also prevents the warm-water from the NECC to reach the Panama Bight. Conversely, in August, the northeast Trade winds are weaker (the southeast Trade winds stronger) and the NECC reaches the Panama Bight. Due to the stronger influence of the southeast Trade winds, upwelling is a common phenomenon in the EEP in August (e.g. Wyrkti, 1974). The NEC and SEC are fed by the south-flowing California Current and the north-flowing Peru Current respectively.

Upwelling caused by divergence (Ekman transport) is an important component of the SEC and affects the uppermost 200 m of the water column. Even though, the vertical speed of water is only 0.02 mh^{-1}, -a rather low speed compared to other coastal upwelling regions-, the net transport of water reaches ~47 Sv (e.g. Wyrtki, 1981; Tomczak and Godfrey, 1994). Upwelling, -though weaker-, is also a common phenomenon in the center of the Panama Bight and the eastern side of the Gulf of Panama during February-March when it moves at a speed of $45x10^{-4}cms^{-1}$ (Stevenson, 1970). Upwelling in the Panama Bight results in a primary production that ranges between 100 to 900 $mgCm^{-2}d^{-1}$ (Bishop and Marra, 1984; Bishop et al., 1986).

The NECC originates in the western Pacific Ocean and transport 45 Sv in the west to 10 Sv east of the Galapagos. The NECC ends in the Costa Rica Dome where the thermocline depth is minimum (e.g. Wyrtki, 1964). The SECC transport ~10 Sv of water at a speed of 0.3 ms^{-1} (e.g. Tomczak and Godfrey, 1994).

At the eastern extreme of the NECC (the Panama Bight), the north-flowing Colombia Current has a speed of 100cms^{-1} in August and 60cms^{-1} in February (e.g. Stevenson, 1970). The latter in response to negative effect of the stronger northeast Trade winds by that time of the year. The Colombia Current has an average

width of 108 km and follows a cyclonic path (e.g. Stevenson, 1970). The boundary between the cold (15º-19ºC), saline (35 p.s.u., i.e. practical salinity units) west-flowing SEC and the warm (>25ºC), fresher (<33.5 p.s.u.) east-flowing NECC constitutes a sharp boundary refer to as the Equatorial Front (e.g. Okuda et al., 1983; Fig. 1a).

Thewing Equatorial undercurrent (EUC), or the Cromwell Current, runs along the equator at 200 m and 40 m water depth in the western and EEP respectively (Fg. 1b). The EUC is 400 km wide, 200 m thick, has a speed of 1.5 ms-1, and t[ra]nsports ~8 Sv of water of southern hemisphere origin (e.g. Toggweiler et al., 1989; Tomczak and Godfrey, 1994). The transport of water by the EUC increases towards the east where it reaches 35-40 Sv (e.g. Tomczak and Godfrey, 1994). The EUC can be identified by the deflection of isotherms and a salinity maximum. The EUC is stronger during January-June and weaker during July-December (e.g. Tomczak and Godfrey, 1994).The Equatorial Intermediate Current (EIC) transport 7±4.8 Sv of water with speeds between 0.1 and 0.2 ms-1 and oc[cu]rs at water depths between 300 and 900m (Fig. 1b). Closely related to the EIC, at 600 m in both hemispheres, occur the North and South Subsurface Countercurrents (NSCC and SSCC). The former countercurrent seems to play an important role in the formation of the Costa Rica Dome (e.g. Tomczak aTomczak and Godfrey, 1994).

The meridional shift of the Intertropical convergence zone (ITCZ), between 9ºN in August and 1ºS in February, causes changes in SST and salinity (SSS). Average SST in March reaches <28ºC northwest of the Panama Bight and <24ºC in front of Guayaquil (Levitus et al., 1994; Fig. 2a). Conversely, in September, the 28ºC isotherm moves to the northeast, whereas a minimum of 21ºC is found in the southwest (at 2ºS; Fig. 2b). The maximum SST gradient is found at 4ºN in September, thus reflecting the position of the Equatorial Front. Seasonal SST patterns for shorter time scales can differ markedly from the Levitus´s et al. (1994) atlas, i.e. the 1970 to 1996 SST average from Colombian Navy cruises (Tchantsev and Cabrera, 1998). The mixed-layer depth, - defined as the depth where water temperature is 5ºC lower than SST (Levitus et al., 1994)-, does not correspond to SST seasonal patterns (Fig. 2c, d). The mixed-layer is >10m deep in the northwest in March and >22m deep between 2 and 4ºN and south of the Equatorial Front in September (Fig. 2c, d)

Average SSS shows a minimum of 31 p.s.u. in the eastern Panama Bight at 4ºN, i.e. west of the San Juan delta, and maximum values (33.5 p.s.u.) in the northwest and southwest of the Bight during March (Fig. 2e; Levitus et al., 1994). This SSS pattern is maintained in September (Fig. 2f). However, extreme values reach 30 p.s.u. and 34.5 p.s.u. respectively (Levitus et al., 1994). The SSS delineation of the Equatorial Front is rather poor. This is not the case of annual dissolved oxygen and AOU (apparent oxygen utilization) that display a sharp contrast at 3ºN reflecting the position of the Equatorial Front (Fig. 3a, c). Oxygen values are >4.7 ml^{-1} west of 86ºW and <4.4 ml^{-1} at 1ºN in the eastern Panama Bight in March, and <0.1 ml^{-1} north of 3ºN with a maximum of >0.5 ml^{-1} at 2ºS in September (e.g. Okuda et al., 1983; Levitus et al., 1994). Similarly, AOU is minimum in the northwest (-0.15) and maximum in the southeast at 1ºN (0.25) for March, and <0.1 north of 3ºN and exceeds 0.5 south of the equator for September (Levitus et al., 1994).

Nitrate (NO_3), phosphate (PO_4), silica (SiO_2) and density (Fig. 3b, d, e, f) also display a strong meridional contrast through the Equatorial Front, i.e. high values in the cold, saline, west-flowing SEC, and low

values in the warm, fresher, east-flowing NECC (e.g. Okuda et al., 1983). Chorophyll and carbon fixation at 10m water depth and PO_4 at 20m also display maximum values, i.e. 30 $mgm^{-3}d^{-1}$, 0.8 mgm^{-3}, and 2 ml^{-1} respectively, south of the Equatorial Front in February (e.g. Forsbergh, 1969).

MATERIALS AND METHODS

A set of 3 cc twenty one core-top samples were obtained from the core repositories of the University of Rhode Island (cores TR), Lamont Doherty Earth Observatory (cores VM), and the Ocean Drilling Program (cores ODP; Table 1). Supplemented information was added from six core-top samples (RC23-12, -20, -113, -138, RC6-69, and VM17-44) from Faul et al. (2000) study. Samples from Cortes et al. (1990) could not be compared due to taxonomic inconsistencies. Core-top samples are assumed to represent the Present, though due to mixing by benthonic organisms they represent the last few hundred years. Core-top samples were recovered from 1700 and 3500 m water-depth. Samples collected below ~2800 m, i.e. the sedimentary lysocline (e.g. Thunell et al., 1981), are more affected by carbonate dissolution.

Samples were soaked in water and diluted hydrogen peroxide until reaction stopped. Wet sieving followed in the 63 and 150 μm size fractions, and drying of the sample at ~40ºC. Counting of specimens was done on a sub-sample of ~300 specimens obtained with the aid of an Otto microsplitter in the >150 μm size fraction.

We follow in this paper a conservative approach to taxonomy thus grouping a number of species as variants of more well-known species (e.g. Parker, 1962, and Plate 1). This assumption might be imprecise as recent DNA sequencing studies have evidenced the existence of cryptic species of planktonic foraminifera undistinguishable on morphological basis (e.g. Pawlowski, 2000; Darling et al., 2000). Dissolution of planktonic foraminifera (percentage abundance) was evaluated by counting the number of fragments over the number of whole specimens.

Species assemblages were obtained by cluster analysis and diversity determined by the Shannon index (MVSP multivariate statistical package), whereas environmental variables were obtained from the World Ocean Atlas available on the Internet (Levitus et al., 1994)

RESULTS

Table 2 contains the percentage abundance of planktonic foraminifera, whereas Figure 4 shows their geographic distribution (percentage abundance) in the EEP Ocean. *Neogloboquadrina dutertrei* is the dominant species in the region showing higher percentage abundances south of the Equatorial Front. *Globigerina bulloides* and *Globigerinita glutinata* are more abundant toward the northwest, as it is *Globorotalia cultrata*, although the latter species is more abundant over the Cocos Ridge, i.e. close to the Costa Rica Dome. *Globigerinoides ruber* and *Globigerinoides sacculifer* show maximum values between the

equator and 6ºN, though the former species concentrates over the Cocos Ridge away from the influence of the Costa Rica Dome. *Globorotalia inflata* is restricted to the region close to Ecuador (over the eastern Carnegie Ridge), whereas *Neogloboquadrina pachyderma* right-form is more abundant southeast of Galapagos Islands and over the Cocos Ridge between 4º and 6ºN.

Fragmentation of planktonic foraminifera is significant in most of the core-top samples and is >70% between the equator and 2ºN and in the northwest north of 5ºN. This fragmentation distribution biases the percentage abundance of solution-susceptible and solution-resistant planktonic foraminiferal species, i.e. *P. obliquiloculata* and *G. cultrata*. Because fragmentation of planktonic foraminifera is linearly related to water depth, we should expect the Shannon diversity index, evenness, and the number of species to show a systematic relation with water depth. Shannon diversity index shows two populations that increase with water depth (Fig. 5a). These two tendencies appear to be related to latitude. However, a change in the number of species with water depth is less evident (Fig. 5b).

Shannon diversity index, evenness, and the number of species increase northwards (Figs. 5c, d and 6). This trend reflects a meridional environmental gradient that controls species distributions. However, there is a major break at ~1.5ºS that roughly corresponds to the Equatorial Front (Figs. 5c, d).

Three bioprovinces are distinguished by Q-mode Cluster Analysis, unweighted pair group average (UPGMA) with an Euclidian distance coefficient (Fig. 7a). Bioprovince I includes samples along the Cocos Ridge; bioprovince II includes samples along the Carnegie Ridge, south of the Equatorial Front; and bioprovince III includes samples from the Panama Basin (Fig. 7b). Even though samples collected over the Cocos and Carnegie Ridges are shallower than those collected on the Panama Basin, there is not a systematic relationship of cluster bioprovinces with water depth, e.g. sample VM19-27 was collected at 1300 m water depth in the Panama Basin and is grouped in bioprovince III rather than II.

DISCUSION

The distribution of planktonic foraminifera in deep-sea sediments of the Panama Basin greatly differs from their distribution in sediment-trap samples. Despite the different mesh sizes used in deep-sea sediment and sediment-trap studies, i.e. >150μm in this study and >330μm (Be et al., 1985) and >125μm (Thunell and Reynolds, 1984), it is evident that dissolution significantly alters planktonic foraminifera assemblages by eliminating the most fragile species. As already noted by Be et al. (1985) *Globorotalia theyeri* and *G. ruber* are dominant in sediment-trap samples collected at ~5ºN-81ºW from the uppermost 2000 m of the water column during July- August as compared to *N. dutertrei* that is dominant in deep-sea sediment samples. Nonetheless, sediment-trap samples collected at the same location do not show major differences in the flux of plantktonic foraminifera at 890, 2590, and 3560m (Thunell and Reynolds, 1984), thus suggesting that despite a foraminiferal lysocline located at ~2800m dissolution in the water column is ineffective in destroying planktonic foraminifera (Thunell and Reynolds, 1984). This contrasts with dissolution at the seafloor where the loss in carbonate is

estimated to be ~84% (Thunell and Reynolds, 1984). This figure is in agreement with previous estimates of ~50% dissolution at ~1500 m, 80% at ~1750 m, and the carbonate compensation depth (CCD) at ~3400 m (Kowsmann, 1973). This shallower lysocline and CCD, when compared with more oceanic regions, is greatly due to an excess of organic matter rain to the seafloor that results in carbonic acid (H_2CO_3) in pore water. When comparing the annual average percentage of planktonic foraminifera from a sediment-trap (5.35ºN, 81.88ºW) collected by Thunell and Reynolds (1984) during a year period from December 1979 with ODP84 (5.75ºN, 82.89ºW) core-top sample reported here (Fig. 8), it appears that *G. glutinata*, *G. ruber* and *G. bulloides* are more abundant in the former than in the latter sample. Conversely, *N. dutertrei*, *G. cultrata*, and *N. pachyderma* are more abundant in the ODP84 core-top sample. As expected the most solution-susceptible species were eliminated from the sediment sample. Nonetheless, part of the difference could be due to other causes different to carbonate dissolution as follows: (1) for Figure 8 the 1979-1980 percentage average in sediment-trap samples was considered rather than the whole range of percentage variation; this is the case for *N. dutertrei* in sediment-trap samples that reaches a maximum value of 59.9% very close to the one determined for the ODP84 core-top sample, (2) the 1979-1980 period represents only a discrete time slice when compared to the centennial character of sediment samples and, (3) species like *G. quinqueloba* were not observed in the core-top sample due to its reduced size <150μm.

Rutherford et al. (1999) have found that diversity of planktonic foraminifera is related to the structure of the upper-water column (the thermocline depth) rather than to SST. Consequently, the largest diversity of planktonic foraminifera occurs at mid latitudes (central gyres) rather than the equatorial regions. This "hump-shape" pattern, - also reported for a number of animal and plant species -, suggesting that diversity is controlled by productivity (e.g. Rosenzweig and Abramsky, 1993). However, an excess of productivity results in low diversity. As for the present data set, south of the Equatorial Front productivity is in excess and diversity therefore decreases thus representing the upper extreme of the "hump-shape" pattern. As with Rutherford et al.'s (1999) global map, the diversity map presented herein (Fig. 6) shows that diversity decreases when the thermoclina is shallow. However, different to Rutherford et al.'s (1999) results, dissolution prevents to establish a relationship between SST and diversity that might help to reconstruct paleo-SSTs from deep-sea cores. In the best case, the major change in diversity at ~1.5ºS might help to reconstruct the past position of the Equatorial Front, i.e. the record of any abrupt down-core changes in the Shannon diversity index for cores located close to the equator.

The species *G. bulloides*, *G. cultrata*, *G. glutinata* and *N. dutertrei* have already been reported as associated to the equatorial "cold-tongue" in contrast to *G. sacculifer*, *G. ruber* and *G. conglobatus* that are associated to subtropical regions (e.g. Watkings et al., 1998). The former species are either symbiont barren or symbiont facultative (diatoms- or chrysophytes-bearing) and mostly herbivorous, whereas the latter species are dinoflagellate bearing and mostly carnivorous (e.g. Hemleben et al., 1989). Diatoms as a base of the food web are replaced by dinoflagellates during El Niño years (e.g. Rojas de Mendiola et al., 1985). This must be

reflected in the presence of abundant *G. sacculifer*, *G. ruber* and *G. conglobatus* during El Niño years in the EEP.

The distribution of cluster bioprovinces I and II from the EEP corresponds to phytoplankton production levels in excess of 700 mgC/m^2/day (Owen and Zeitzschel, 1970). These high productivity levels result from upwelling thus favoring the presence of *G. cultrata* and *N. pachyderma* in the north (around the Panama Bight and the Costa Rica Dome) and *N. dutertrei*, *N. pachyderma* and *G. inflata* south of the Equatorial Front. The difference is due to upwelling intensity that results in different food webs (e.g. Owen and Zeitzschel, 1970; Honjo, 1982).

The distribution of cluster bioprovince III from the Panama Basin coincides with a maximum abundance of benthonic foraminifera and bivalve larvae collected from filtered water samples (Thiede, 1983). *Rosalina globularis* is the most abundant benthonic foraminifera species. *R. globularis* develops an ephemeral floating chamber before sexual reproduction; therefore its abundance in the central Panama Basin is used as a proof of drifting from coastal regions as the species is epi-benthic and lives in shallow waters (Thiede, 1983). A similar reasoning applies to the bivalve larvae whose abundance increases shoreward (Thiede, 1983). As noted by Thiede (1983), these dispersal patterns could be related to the Colombian Current. Subsurface currents might be involved in their re-distribution either by supplying nutrients or by passively carrying benthonic foraminifera and bivalve larvae along their path, i.e. the Equatorial Underwater Current or the Cromwell Current whose path in the Panama Basin (Pineda, 1997) resembles the distribution of bivalve larvae.

Globorotalia inflata is a species dominant in transitional regions between the subtropics and the poles (20 to 60^{o}S), lives in deep waters under the thermocline (>100 m), shows a wide range of tolerances to temperature and salinity and can facultatively host photosynthetic symbionts in their protoplasm (e.g. Hemleben et al., 1989; Hilbrecht, 1996). However, the species was found in TR163-38 core-top sample about 14^o north of the nearest reported occurrence in core-top sample V19-41 (14.1^{o}S; 96.1^{o}W; Thompson, 1976). This might imply that episodic pulses of the Peru Current could carry *G. inflata* significantly north of its normal habitat.

South of the Equatorial Front, and co-occurring with sediment samples that provide abundant *N. dutertrei*, *N. pachyderma* and *G. inflata*, plankton tow collections provide abundant diatoms, coccolithophorids (mainly *Emiliana huxleyi*), copepods and euphausiids, among others (e.g. Jimenez and Bonilla, 1980; Bishop et al., 1986). *N. dutertrei*, *N. pachyderma* and *G. inflata* are symbiont-barren and live deep in the water column, thus suggesting that they should prey on diatoms and coccolithophorids and be consumed by copepods and euphausiids. Conversely, north of the Equatorial Front, dinoflagellates and chaetognaths co-occur with G. *sacculifer*, *G. ruber*, and *G. glutinata*. These species are symbiont-bearing or symbiont-facultative and preferentially should prey on dinoflagellates and are consumed by chaetognaths among other groups. At the Panama Bight diatoms and silicoflagellates are the dominant phytoplankton groups in the >53µm size-fraction whereas copepods, larvaceans, chaetognaths and ostracods are the

dominant zooplankton in the >333μm size-fraction during July-August, i.e. after the upwelling event (Bishop et al., 1986). During July-August planktonic foraminifera in the >333μm size-fraction were more abundant than during November-December presumably due to the elevated supply of food and/or more predation on the smaller foraminifera (Bishop et al., 1986).

Even though, coastal and equatorial upwelling of sub-surface water have been suggested to be the main mechanisms responsible for vertical mixing and the supply of nutrients to the mixed layer of the EEP, vertical mixing could also result south of the Carnegie Ridge where a rough topography might prevent the free northward flow of deep-water currents. This mechanism, - documented elsewhere (Brazil abyssal plain) -, and has been suggested to account for the closing of global overturning circulation following the formation of deep-water in high latitudes and horizontal transport of ocean currents (Ledwell et al., 2000).

CONCLUSIONS

Despite the intense carbonate dissolution which significantly affects the preservation of planktonic foraminifera assemblages deposited on the seafloor in the EEP, there are a number of observations that can be used in paleoceanographic reconstruction as follows:

1) Because of carbonate dissolution, induced by the corrosiveness of deep water and intense organic matter rain to the seafloor, there is an anomalous increase of the solution-resistant species *N. dutertrei*, *N. pachyderma* and *G. cultrata* and a reduction of *G. glutinata*, *G. ruber* and *G. sacculifer* in deep-sea sediments with respect to sediment-trap samples.
2) Three bioprovinces were recognized on the EEP by cluster analysis: (a) bioprovince I that occurs on the Cocos Ridge where *G. cultrata* and *N. pachyderma* are dominant, (b) bioprovince II that occurs on the Carnegie Ridge where *N. dutertrei*, *N. pachyderma* and *G. inflata* are dominant, and (c) bioprovince III that occurs in the Panama Basin where *G. sacculifer* and *G. ruber* are dominant.
3) Bioprovinces I and II do reflect a shallow thermocline induced by upwelling (Costa Rica Dome - Panama Bight and equatorial divergence), although AOU, NO_3 and PO_4 and SiO_2 are significantly higher in the latter region. Bioprovince III reflects a deep-mixed layer and low nutrient contents.
4) The occurrence of *G. inflata* in core-top sample TR163-38 suggests the episodic inflow of the Peru Current thus transporting this subtropical species into the Panama Basin.
5) Two possible proxies of the Equatorial Front in the past are suggested: (a) the Shannon diversity index, evenness and the number of species that show a latitudinal break at ~1.5ºS and, (b) the *G. cultrata* / *G. dutertrei* ratios that decrease southward.

ACKNOWLEDGEMENTS

This work is part of the research project: “Late Quaternary paleoceanography of the Panama Basin, Colombian Pacific: Implications for Global Climate Change” funded by Universidad EAFIT – COLCIENCIAS (Programa Nacional de Medio Ambiente y Habitat). We thank Dr. John Firth (*Ocean Drilling Program*) and Dr. Steven Carey (University of Rhode Island, NSF grant OCE-9102410) for kindly providing the core-top samples and Julliet Betancur for diligently processing the samples. Maria Isabel Acevedo and Wilton Echavarria are acknowledged for their logistic support. Christina Ravelo kindly provided foraminifera countings from six core-top samples (Faul et al., 2000 study). We thank Georges Vernette for a careful review of the manuscript.

REFERENCES

Anderson, D. M., Prell, W. L., and N. J. Barrat. 1989. Estimates of sea surface temperature in the Coral Sea at the last glacial maximum. Paleoceanogr., 4:615-627.

Be, A. W. H., Bishop, J. K. B., Sverdlove, M. S. and W. D. Gardner. 1985. Standing stock, vertical distribution and flux of planktonic foraminifera in the Panama Basin. Marine Micropaleontology 9, 307-333.

Bishop, J. K. B. and J. Marra. 1984. Variations in primary production and particulate carbon flux through the base of the euphotic zone at the site of the Sediment Trap Intercomparison Experiment (Panama Basin). J. Mar. Res., 42:189-206.

Bishop, J. K. B., Stephen, J. C. and P. H. Wiebe. 1986. Particulate matter distributions, chemistry and flux in the Panama Basin: Response to environmental forcing. Prog. Oceanog. 17:1-59.

Broecker, W. S. and G. H. Denton. 1989. The role of ocean-atmosphere reorganizations in glacial cycles. Geochim. Cosmochim. Acta, 53:2465-2502.

CLIMAP Project Members, 1976. The surface of the ice-age earth. Science, 191:1131-1137.

Cortes, E. A., Bulla, J. G. and C. Parada. 1990. Foraminíferos planctónicos en sedimentos superficiales del Pacifico Colombiano. VII Seminario Nacional de las Ciencias y Tecnologías del Mar, Memorias, 210-223.

Darling, K. F., Wade, C. M., Steward, I. A., Kroon, D., Digle, R. and A. J. Leigh. 2000. Molecular evidence for genetic mixing of Arctic and Antarctic subpolar populations of planktonic foraminifers. Nature, 405:43-47.

Fairbanks, R. G., Sverdlove, M., Free, R., Wiebe, P. H. and A. W. H. Be. 1982. Vertical distribution and isotopic fractionation of living planktonic foraminifera from the Panama Basin. Nature, 298:841-844.

Faul, K. L., Ravelo, A. C. and M. L. Delaney. 2000. Reconstructions of upwelling, productivity and photic zone depth in the eastern equatorial Pacific Ocean using planktonic foraminiferal stable isotopes and abundances. J. Foram. Res. 30(2):110-125.

Forsbergh, E. D. 1969. On the climatology, oceanography and fisheries of the Panama Bight. - Inter-Amer. Trop. Tuna Comm. Bull., v. 30, p. 141-170.

Hemleben, G., Spindler, M. and R. O. Anderson. 1989. Modern Planktonic Foraminifera. Springer, New York, 363 p.

Hilbrecht, H. 1996. Extant planktonic foraminifera and the physical environment in the Atlantic and Indian Oceans – An Atlas based on CLIMAP and Levitus (1982) data. Mitt. Geol. Inst. Eidgen. Tech. Hochschule and Univ. Zurich N. F. 300, 93 p.

Honjo, S. 1982. Seasonality and interaction of biogenic and lithogenic particulate flux at the Panama Basin. Science, 218:883-884.

Jimenez, R. and D. Bonilla. 1980. Composicion y distribucion de la biomasa del plancton en el Frente Equatorial. Acta Oceanográfica del Pacifico INOCAR, 1(1):19-64.

Kowsmann, R. O. 1973. Coarse components in surface sediments of the Panama Basin, eastern equatorial Pacific. J. Geol., 81:473-494.

Ledwell, J. R., Montgomery, E. T., Polzin, K. L., Laurent, L. C. St., Schmitt, R. W. and J. M. Tole. 2000. Evidence for enhanced mixing over rough topography in the abyssal ocean. Nature, 403:179-182.

Levitus, S., Burgett, R. and P. Boyer. 1994. World Ocean Atlas. NOAA, US Dept. Commerce, Washington D.C. Homepage: http://ingrid.ldgo.columbia.edu/SOURCES/.LEVITUS94/.

Lonsdale, P. E. and B. T. Malfait. 1974. Abyssal dunes of foraminiferal sand on the Carnegie Ridge. GSA Bull., 85:1697-1712.

Mix, A. C., Morey, A. E., Pisias, N. G. and S. W. Hostetler. 1999. Foraminiferal faunal estimates of paleotemperature: Circumventing the no-analog problem yields cool ice age tropics. Paleoceanogr., 14(3):350-359.

Okuda, T., Suescum, R. T., Valencia, M. and A. Rodriguez. 1983. Variación estacional de la posición del Frente Ecuatorial y su efecto sobre la fertilidad de las aguas superficiales ecuatorianas. Acta Oceanográfica del Pacifico INOCAR, 2(1):53-84.

Owen, R. W. and B. Zeitzschel. 1970. Phytoplankton production: seasonal change in the oceanic eastern tropical Pacific. Mar. Biol., 7:32-36.

Pak, H. and J. R. V. Zaneveld. 1974. Equatorial Front in the eastern Pacific Ocean. J. Phys. Oceanogr., 4:570-578.

Parker, F. L. 1962. Planktonic foraminiferal species in Pacific sediments. Micropaleontology, 8(2):219-254.

Pawlowski, J. 2000. Introduction to the molecular systematics of foraminifera. Micropaleontology, 46(1):1-12.

Pineda, A. R. 1997. La Corriente de Cromwell durante el fenómeno de La Niña de 1996 y el fenómeno de El Niño de 1997, sobre la Cuenca del Pacifico Colombiano. CCCP Boletín Científico, Armada Nacional (Colombia), 6:109-122.

Pisias, N. G. and A. C. Mix. 1997. Spatial and temporal oceanographic variability of the eastern equatorial Pacific during the late Pleistocene: Evidence from radiolarian microfossils. Paleoceanography, 12:381-393.

Rojas de Mendiola, B., Gomez, O. and B. Ochoa. 1985. Identificación del fenomeno “El Niño” a traves de los organismos fitoplanctónicos. Bol. Instituto del Mar del Peru:23-31.

Rosenzweig, M. L. and Z. Abramsky. 1993. How are diversity and productivity related? In: R. E. Ricklefs, D. Schluter (eds.) Species Diversity in Ecological Communities: Historical and Geographical Perspectives. Univ. Chicago Press, 52-65.

Rutherford S., D’Hont, S. and W. Prell. 1999. Environmental controls on the geographic distribution of zooplankton diversity. Nature, 400:749-752.

Stevenson, M. 1970. Circulation in the Panama Bight. J. Geoph. Res., 75(3):659-672.

Tchantsev, V. and E. Cabrera. 1998. Algunos aspectos de investigación de la formación del régimen oceanografico en el Pacifico Colombiano. Boletín Científico CCCP, 7:7-19.

Thiede, J. 1983. Skeletal plankton and nekton in upwelling water masses off northwestern South America and northwest Africa. In: Coastal Upwelling. Its sedimentary record. Art A: Responses of the sedimentary regime to present coastal upwelling (E. Suess, J. Thiede, eds.), Nato, Plenum Press, 183-207.

Thompson, P. R. 1976. Planktonic foraminiferal dissolution and the progress towards a Pleistocene Equatorial Pacific transfer function. J. Foram. Res., 6(3):208-227.

Thunell, R. C., Keir, R. S. and S. Honjo. 1981. Calcite dissolution: An in situ study in the Panama Basin. Science, 212:659-661.

Thunell, R. C., Curry, W. B. and S. Honjo. 1983. Seasonal variation in the flux of planktonic foraminifera: time series sediment trap results from the Panama Basin. Earth Planet. Sci. Letters, 64:44-55

Thunell, R. C. and L. A. Reynolds. 1984. Sedimentation of planktonic foraminifera: Seasonal changes in species flux in the Panama Basin. Micropaleont., 30:243-262.

Toggweiler, J. R., Dixon, K. and K. Bryan. 1989. Simulation in a coarse-resolution world ocean model, 1. Steady state prebomb distributions. J. Geophys. Res., 94, C6:8217-8242.

Tomczak, M. and J. S. Godfrey. 1994. Regional Oceanography: An Introduction. Pergamon, Oxford, 422 pp.

Van Andel, T. H. 1973. Texture and dispersal of sediments in the Panama Basin. J. Geology, 81:434-457.

Watkings, J. M., Mix, A. C. and J. Wilson. 1998. Living planktic foraminifera in the central tropical Pacific Ocean: articulating the equatorial “cold tongue” during La Niña, 1992. Mar. Micropaleont., 33:157-174.

Wooster, W. S. 1969. Equatorial Front between Peru and Galapagos. Deep-Sea Res., 16:407-419.

Wyrkti, K. 1964. Upwelling in the Costa Rica Dome. Fishery Bull., 63(2):355-372.

Wyrkti, K. 1974. Equatorial currents in the Pacific 1950 to 1970 and their relation to trade winds. J. Phys. Oceanogr., 4:372-380.

Wyrtki, K. 1981. An estimate of equatorial upwelling in the Pacific. J. Phys. Oceanogr., 11:1205-1214.

Yamashiro, C. 1975. Differential dissolution and transport effects in foraminiferal sediments from the Panama Basin. Cushman Found. Foram. Res., Spec, Publ., 13:151-159.

For planktonic foraminifera raw data see *Microfossil* homepage (Data link) (http://www.geocities.com/CapeCanaveral/Launchpad/4680/).

AUTHORS’S ADDRESS:

Universidad EAFIT, Departamento de Geología, Grupo de Ciencias del Mar, A.A. 3300 Medellín, Colombia. E-mail jimartin@eafit.edu.co

APPENDIX

Faunal reference list.

Globigerina bulloides d'Orbigny

Globigerina calida Parker

Globigerina digitata Brady

Globigerina falconensis Blow

Globigerinella siphonifera (d'Orbigny)

Globigerinoides conglobatus (Brady)

Globigerinoides elongatus (d'Orbigny)

Globigerinoides ruber (d'Orbigny)

Globigerinoides sacculifer (Brady)

Globoturborotalita rubescens (Hofker)

Globoturborotalita tenella (Parker)

Orbulina universa d'Orbigny

Sphaeroidinella dehiscens (Parker and Jones)

Globigerinita glutinata (Egger)

Globoquadrina conglomerata (Schwager)

Globorotalia crassaformis (Galloway and Follador)

Globorotalia crotonensis Conato and Follador

Globorotalia cultrata (d'Orbigny)

Globorotalia inflata (d'Orbigny)

Globorotalia scitula (Brady)

Globorotalia tumida (Brady)

Globorotalia ungulata Bermudez

Globorotaloides hexagonus (Natland)

Neogloboquadrina dutertrei (d'Orbigny)

Neogloboquadrina pachyderma (Ehrenberg)

Pulleniatina obliquiloculata (Parker and Jones)

EXPLICACION DE LAS FIGURAS

Figure 1. Physical oceanography of the Eastern Equatorial Pacific Ocean: (a) Sea surface currents (in black), the Equatorial Undercurrent (in gray), upwelling (in shading) and core-top locations (asterisks), (b) Structure of the upper-water column along 170ºW; westward currents (in blank) and eastward currents (in hatching). NEC and SEC = North and South Equatorial Currents, EUC = Equatorial Undercurrent, NECC and SECC = North and South Equatorial Countercurrents, SSCC = North and South Subsurface Equatorial Countercurrents and, EIC = Equatorial Intermediate Current. CC = Colombian Current. Note the position of the Equatorial Front. Modified from Tomczak and Godfrey (1994)

Figure 2. Environmental variables on the Eastern Equatorial Pacific Ocean: (a) sea-surface temperature (SST) in March, (b) SST in September, (c) mixed-layer depth (m) for March, (d) mixed-layer depth (m) for September, (e) sea-surface salinity (SSS) for March, (f) SSS for September. Data from Levitus et al. (1994).

Figure 3. Environmental variables on the Eastern Equatorial Pacific Ocean: (a) Apparent oxygen utilization (AOU), (b) nitrate (NO_3) in mmol, (c) dissolved oxygen in ml/l, (d) phosphate (PO_4) in mmol, (e) silica (SiO_2) in mmol and, (f) density. Data from Levitus et al. (1994).

Figure 4. Relative abundance (percentage) of planktonic foraminifera in core-top from the Eastern Pacific: (a) *Globigerina bulloides*, (b) *Globigerinita glutinata*, (c) *Globigerinoides sacculifer*, (d) *Globigerinoides ruber*, (e) *Globorotalia cultrata*, (f) *Globorotalia inflata*, (g) *Neogloboquadrina dutertrei*, (h) *Neogloboquadrina pachyderma*.

Figure 5. Core-top planktonic foraminiferal diversity for the Eastern Pacific: (a) Shannon diversity index and evenness against water depth, (b) number of species against water depth, (c) Shannon diversity index and evenness against latitude, (d) Number of species against latitude.

Figure 6. Shannon diversity index from core-top samples from the Eastern equatorial Pacific Ocean.

Figure 7. Core-top planktonic foraminiferal cluster analyses (UPGMA) for the Eastern Pacific; (a) dendrogram, (b) bioprovinces map. Core-top locations in asterisks.

Figure 8. Comparison of the percentage abundance of planktonic foraminifera from ODP84 core-top sample (in shaded; 5.75ºN, 82.89ºW) and a sediment-trap sample (in blank; 5.35ºN, 81.88ºW; Thunell and Reynolds, 1984).

EXPLICACION DE LAS TABLAS

Table 1. Core-top location for the Eastern Equatorial Pacific Ocean.

Table 2. Percentage abundance of planktonic foraminifera from deep-sea sediments from the Eastern Equatorial Pacific Ocean. For the full species names see the reference list (Appendix).

EXPLICACION DE LA PLANCHA (PLATE 1)

Fig. 1. *Globigerina bulloides* d'Orbigny, umbilical view.

Fig. 2. *Globigerina calida* Parker, umbilical view.

Fig. 3. *Globigerina calida* Parker, dorsal view.

Fig. 4. *Globigerinella siphonifera* (d'Orbigny).

Fig. 5. *Globigerinoides conglobatus* (Brady), umbilical view.

Fig. 6. *Globigerinoides elongatus* (d'Orbigny), umbilical view.

Fig. 7. *Globigerinoides ruber* (d'Orbigny), umbilical view.

Fig. 8. *Globigerinoides ruber* (d'Orbigny), dorsal view.

Fig. 9. *Globigerinoides sacculifer* (Brady), umbilical view.

Fig. 10. *Globoturborotalita rubescens* (Hofter), umbilical view.

Fig. 11. *Globoturborotalita tenella* (Parker), umbilical view.

Fig. 12. *Orbulina universa* d'Orbigny, umbilical view.

Fig. 13. *Globoquadrina conglomerata* (Schwager), umbilical view.

Fig. 14. *Globoquadrina conglomerata* (Schwager), dorsal view.

Fig. 15. *Globorotaloides hexagonus* (Natland), dorsal view.

Fig. 16. *Globorotalia cultrata* (d'Orbigny), umbilical view.

Fig. 17. *Globorotalia cultrata* (d'Orbigny), dorsal view.

Fig. 18. *Globorotalia inflata* (d'Orbigny), umbilical view.

Fig. 19. *Globorotalia inflata* (d'Orbigny), dorsal view.

Fig. 20. *Globorotalia tumida* (Brady), umbilical view.

Fig. 21. *Globorotalia tumida* (Brady), dorsal view.

Fig. 22. *Neogloboquadrina dutertrei* (d'Orbigny), umbilical view.

Fig. 23. *Neogloboquadrina dutertrei* (d'Orbigny), dorsal view.

Fig. 24. *Pulleniatina obliquiloculata* (Parker y Jones), umbilical view.

Fig. 25. *Pulleniatina obliquiloculata* (Parker y Jones), profile view.

Fig. 26. *Neogloboquadrina pachyderma* (Ehrenberg), umbilical view.

Fig. 27. *Neogloboquadrina pachyderma* (Ehrenberg), dorsal view.

Fig. 28. *Sphaeroidinella dehiscens* (Parker and Jones), dorsal view.

Fig. 29. *Globigerinita glutinata* (Egger), dorsal view.

Fig. 30. *Globigerinita glutinata* (Egger), ventral view

Tabla 1. Características merísticas y morfométricas para distinguir entre géneros y estadíos de camarones penéidos. Información tomada de: Cook (1964), Pérez-Farfante (1970), Pérez-Farfante (1988), Reyes (1975).

	Farfantepenaeus spp	***Xiphopenaeus kroyeri***
Postlarvas	**LT:** 6.0 mm – 15.0 mm **Rostrum:** Presenta dientes subrostrales **No. de dientes dorsales del rostrum:** < 7 **Espina Antenal:** Ausente **Telson:** Cinco pares de espinas terminales	**LT:** 6.0 mm ó menos – 14.0 mm **Rostrum:** Sin dientes subrostrales **No. de dientes dorsales del rostrum:** < 5 **Espina Antenal:** Presente **Telson:** Sin espinas terminales
Juveniles	**LT:** > 15.0 mm **Rostrum :** Presenta dientes subrostrales **No. De dientes dorsales del rostrum:** 7 - 10	**LT:** > 14.0 mm **Rostrum:** Sin dientes subrostrales **No. De dientes dorsales del rostrum:** 5

Tabla 2. Información general de las postlarvas (PL) y juveniles (J) de camarones *Farfantepenaeus spp.* y *Xiphopenaeus kroyeri* colectados en la Boca de la Barra (**CGSM**). Febrero 1998 – Febrero 1999.

Taxa	Estadio	Total (No.)	Biomasa Total (g)	LT (mm)	LC (mm)	Espinas dorsales rostrum (No.)
Farfantepenaeus spp.	PL	419	0.7043	6.87– 14.26	1.4 – 3.9	3 – 7
Farfantepenaeus spp.	J	248	411.854	18.12 – 105.75	4.4 – 23.68	7 – 10
Xiphopenaeus kroyeri	PL	206	0.8817	4.0 – 13.75	1.0 – 3.75	2 – 5
Xiphopenaeus kroyeri	J	58	2.8556	14.0 – 43.12	3.85 - 10.75	6 – 8
TOTAL		931	416.30			

Tabla 3. Características merísticas y morfométricas de postlarvas (PL) y juveniles (J) de camarones *Farfantepenaeus spp* y *Xiphopenaeus kroyeri*. Comparación entre diferentes estudios. Los asteriscos indican valores promedio y los datos en paréntesis son el número de espinas dorsales del rostrum más frecuente.

Taxa	Estadio	Longitud Total (mm)	Longitud Caparazón (mm)	Espinas Dorsales Rostrum (No.)	Área de Estudio	Autor y Fecha
P. aztecus/P. brasiliensis	PL	10.5 - 14.0		4 - 7	Florida Keys	Allen *et al.* (1980)
P. duorarum	PL	5.0 - 10.0		2 - 6		
Penaeus spp	PL	7.2 - 10.2		2 - 6 (4,5)	Ciénaga Grande de Santa Marta	Buenaventura y Arango (1980)
	J			6 - 9		
Penaeus spp.	PL	6.0 - 9.0		4 - 7	Ciénaga Grande de Santa Marta	Perea (1981)
Penaeus aztecus	J	6.24*	13.55*		Ciénaga Grande de Santa Marta	Sánchez (1991)
P. duorarum	J	51.37*	11.35*			
P. schmitii	J	55.23*	11.53*			
Farfantepenaeus spp	PL	6.87 - 14.26	1.4 - 3.9	3 - 7 (3,4)	Ciénaga Grande de Santa Marta (Boca de la Barra)	Presente estudio
Farfantepenaeus spp	J	18.12 – 105.75	4.4 – 23.68	7 - 10 (9)		
Xiphopenaeus kroyeri	J	20.0 - 40.0		5	Costa Verde Plataforma Continental Frente a Ciénaga (Magdalena)	Cortés (1989)
Xiphopenaeus kroyeri	PL	4.0 – 13.75	1.0 – 3.75	2 - 5 (4)	Ciénaga Grande de Santa Marta (Boca de la Barra)	Presente estudio
Xiphopenaeus kroyeri	J	14.0 – 43.12	3.85 - 10.75	6 - 8 (5)		

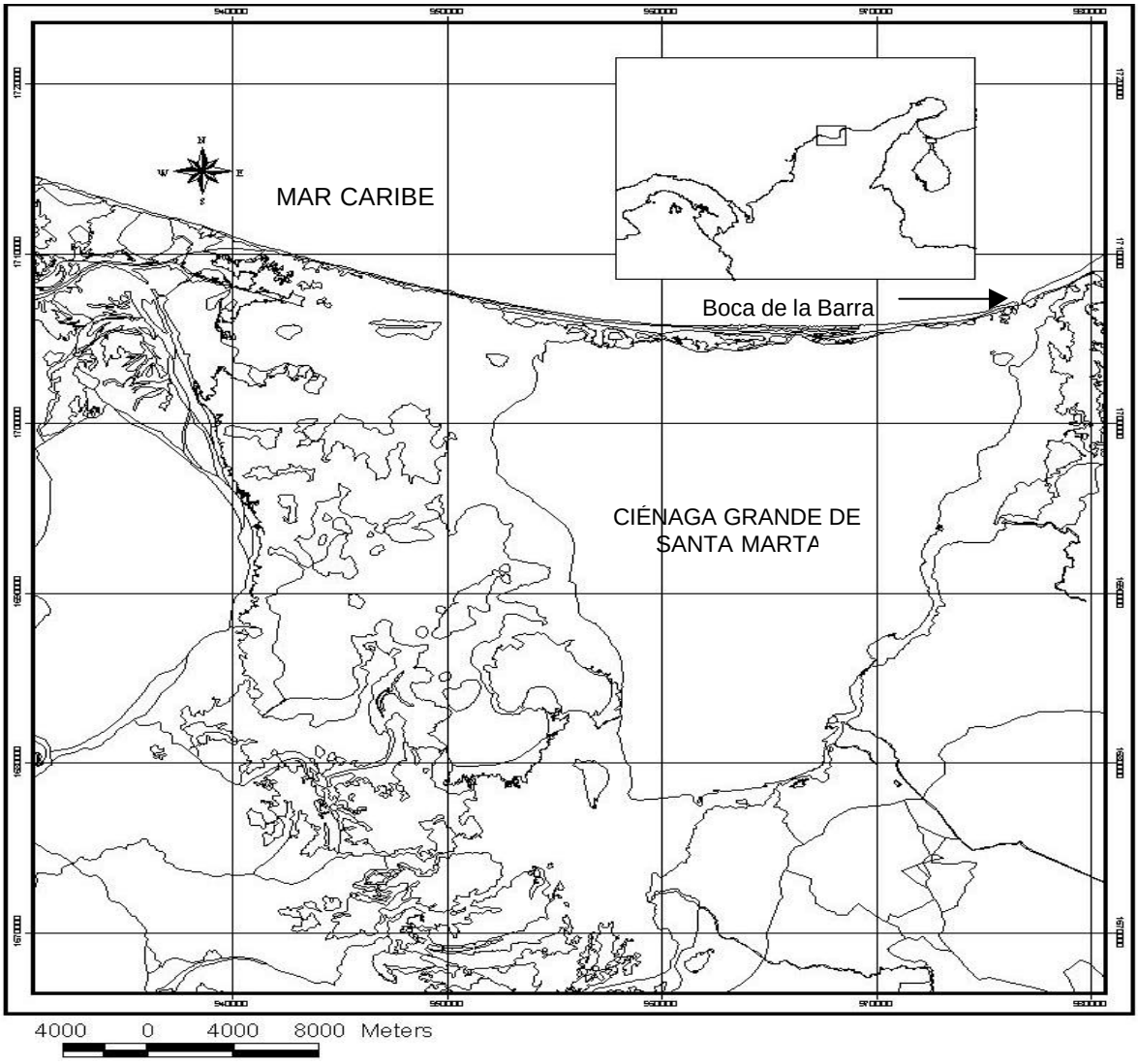

Figura 1. Área de estudio

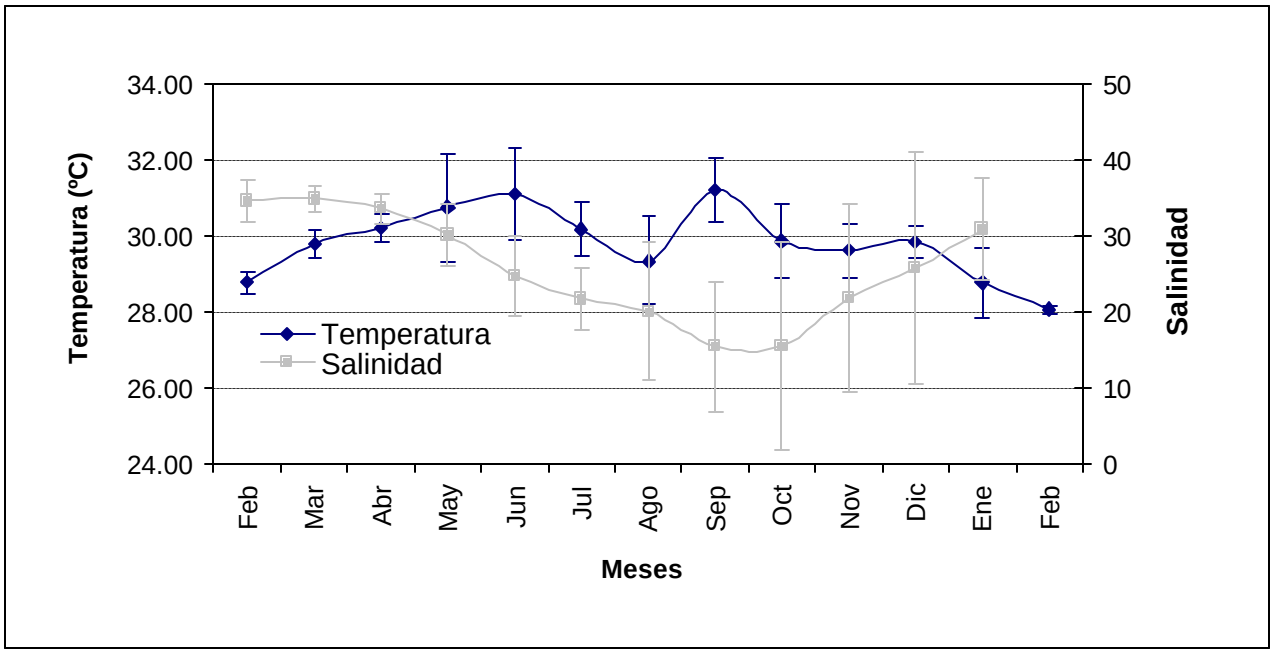

Figura 2. Temperatura y salinidad del agua en la Boca de la Barra. Los valores de temperatura, son el promedio de los registros de esta variable durante los muestreos de este estudio. Los valores de salinidad son promedios mensuales de 7 años, tomados de: Base de datos INVEMAR (1999).

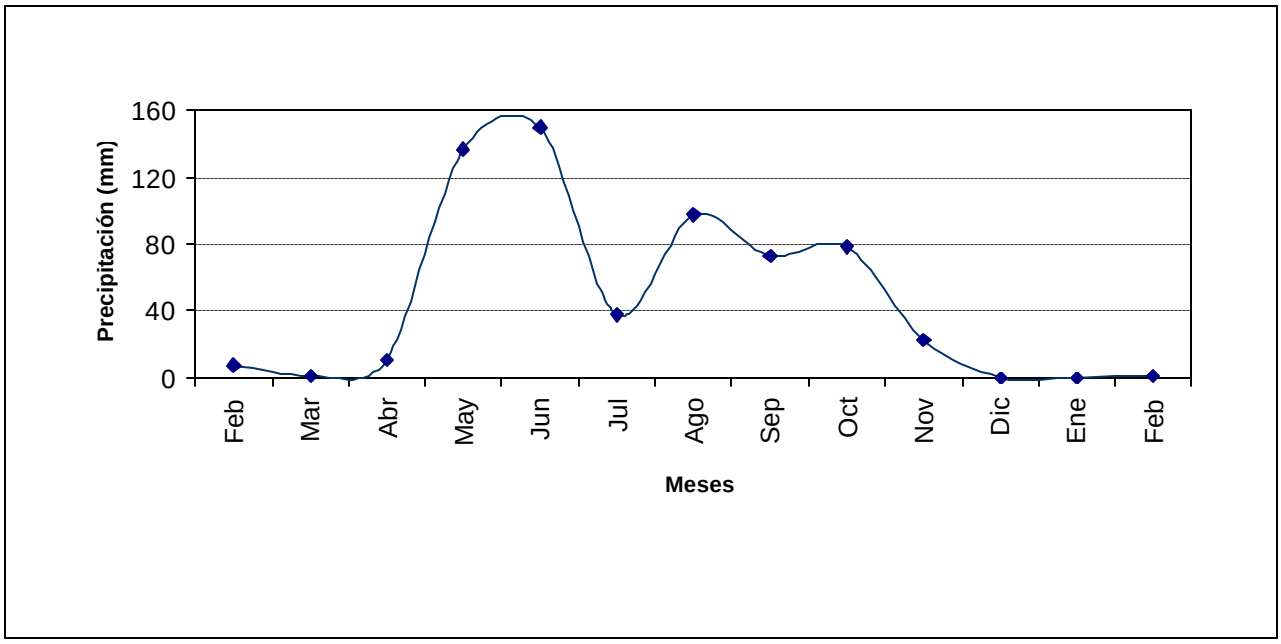

Figura 3. Precipitación total mensual, febrero 1998 - febrero 1999.
Fuente: Estación meteorológica del IDEAM, Aeropuerto Simón Bolívar (Santa Marta).

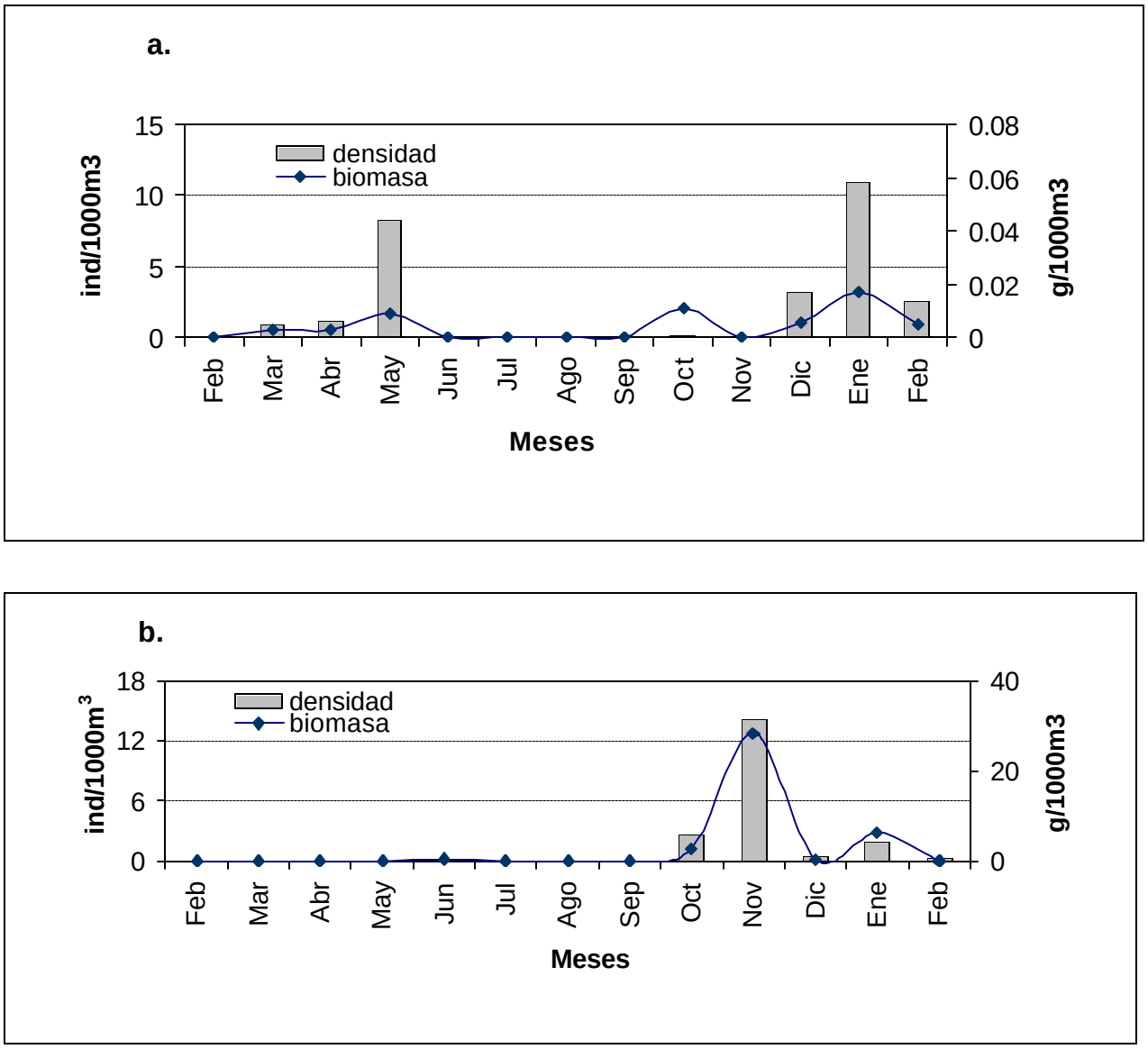

Figura 4. Promedio mensual de densidad y biomasa de los camarones *Farfantepenaeus spp*. colectados en la Boca de la Barra (CGSM), febrero 1998 - febrero 1999. a. Postlarvas y b. Juveniles. Se excluyen las barras de error estandar para dar mayor claridad a los gráficos.

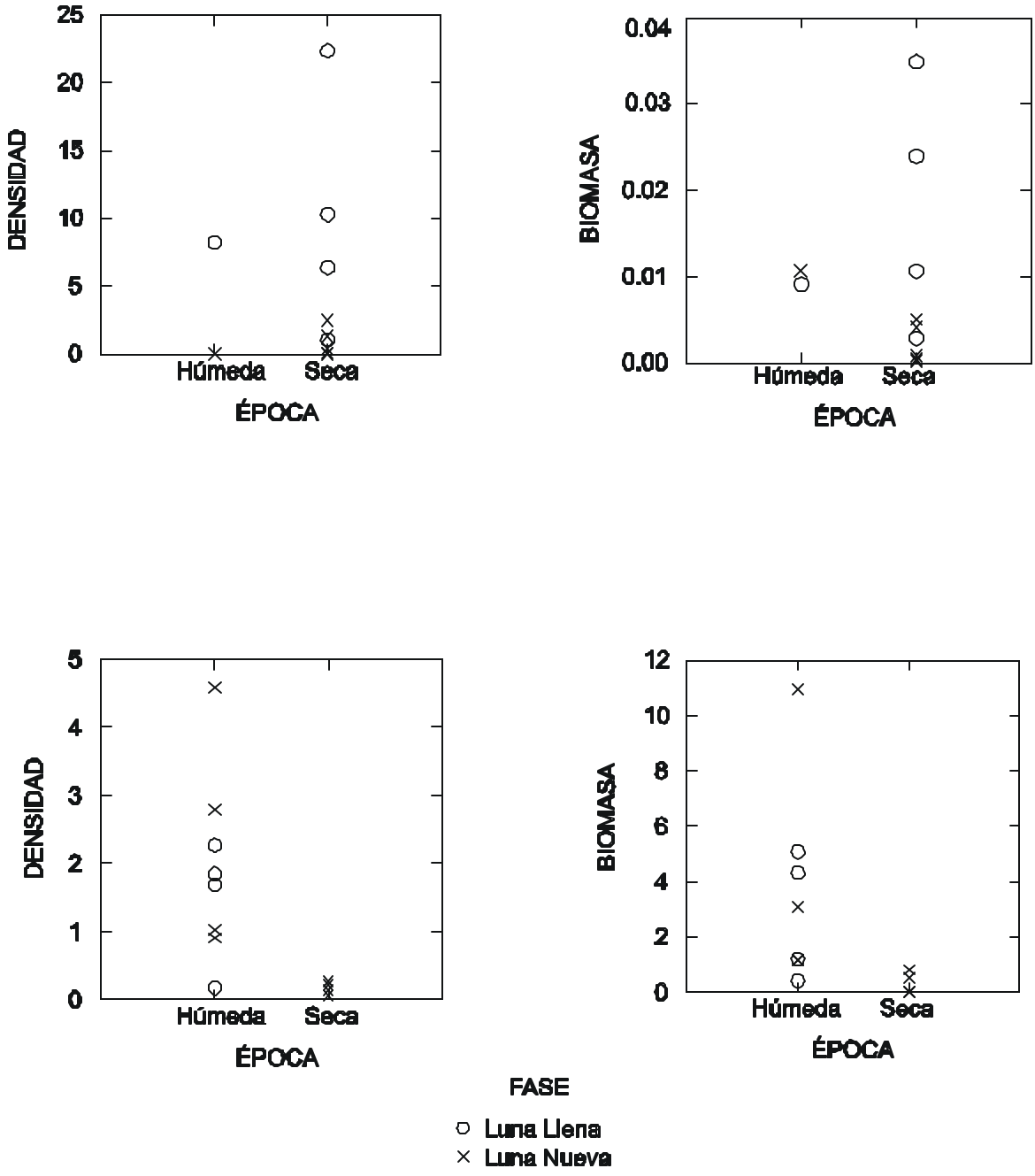

Figura 5. *Farfantepenaeus spp*

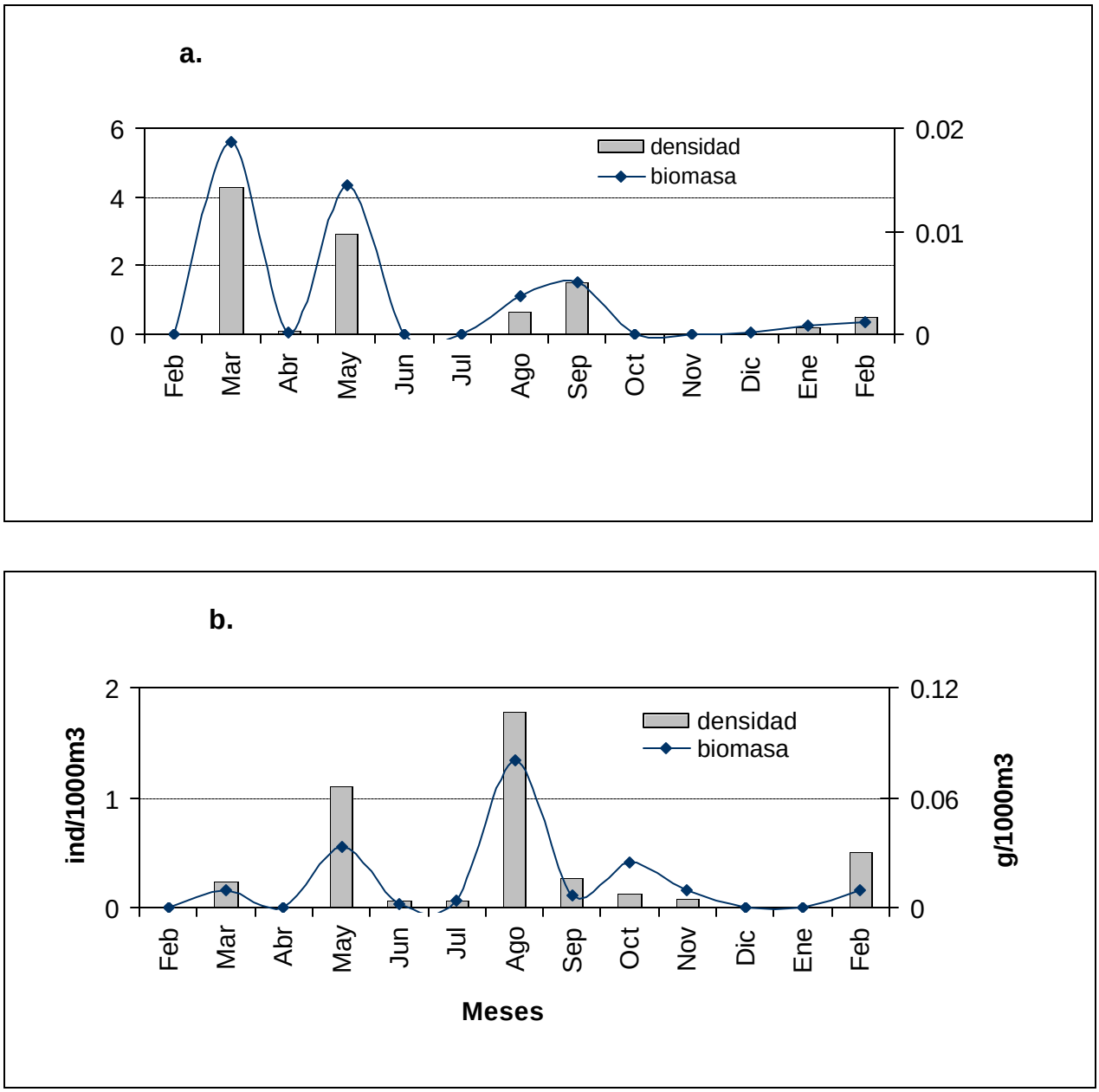

Figura 6. Promedio mensual de densidad y biomasa de camarones *Xiphopenaeus kroyeri* colectados en la Boca de la Barra (CGSM), febrero 1998 - febrero 1999. a. Postlarvas y b. Juveniles. Se excluyen las barras de error estandar para dar mayor claridad a los graficos.

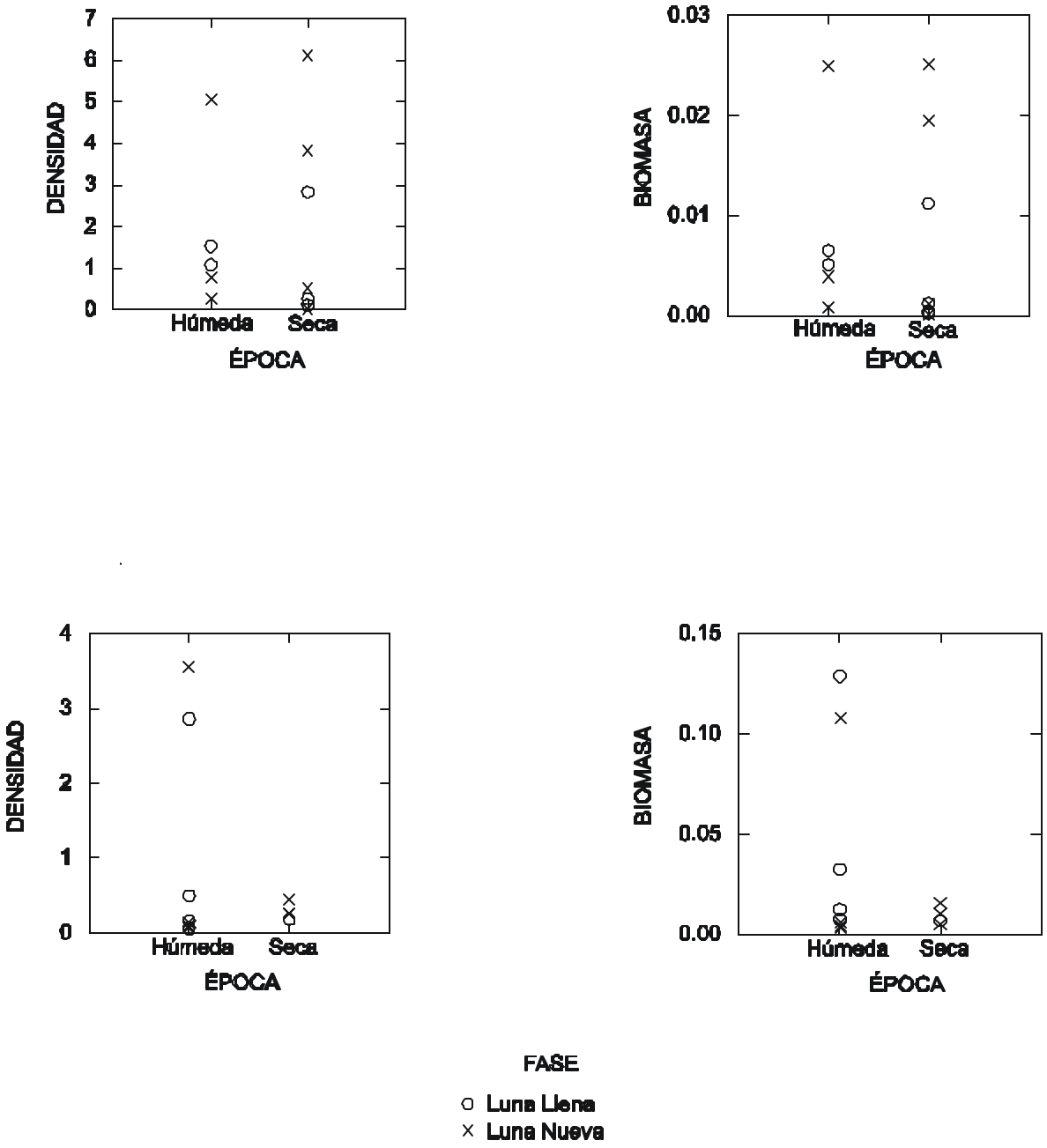

Figura 7. *Xiphopenaeus kroyeri*

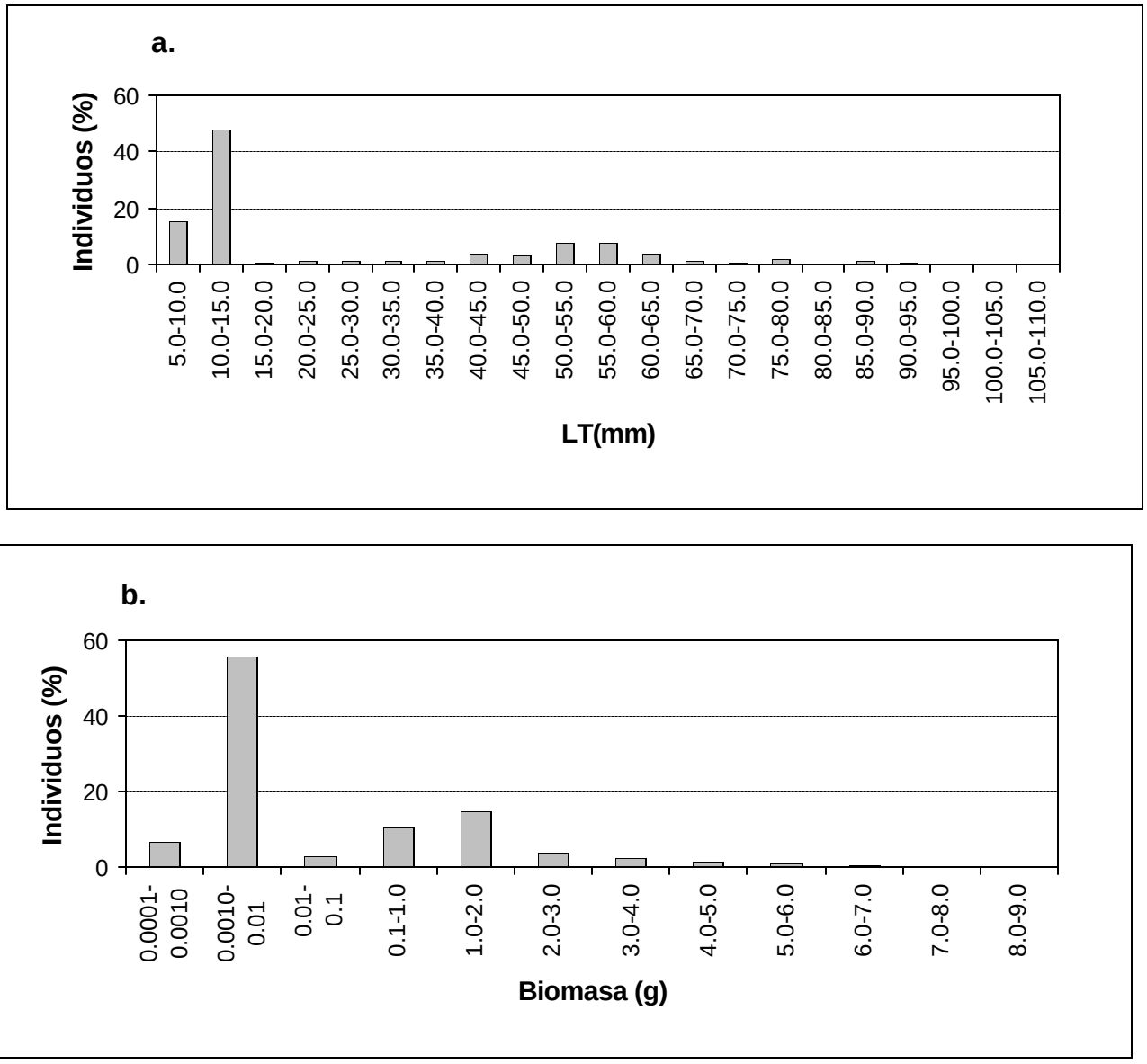

Figura 8. Rangos de longitud total -LT- (a.) y biomasa (b.) , de postlarvas y juveniles de camarones *Farfantepenaeus spp*. Boca de la Barra (CGSM), febrero 1998 - febrero 1999.

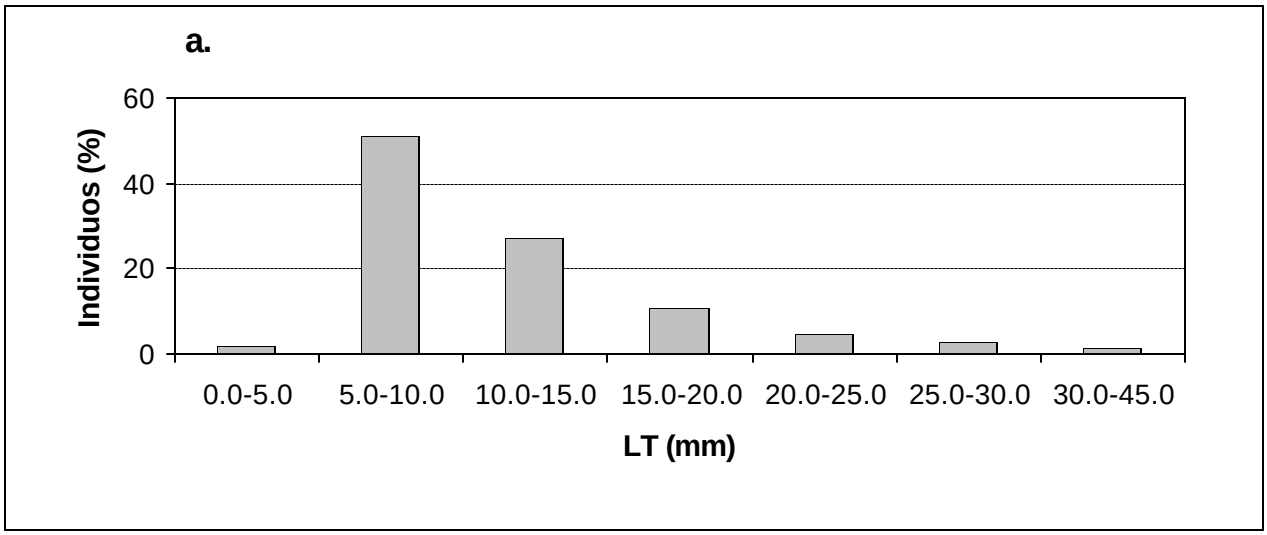

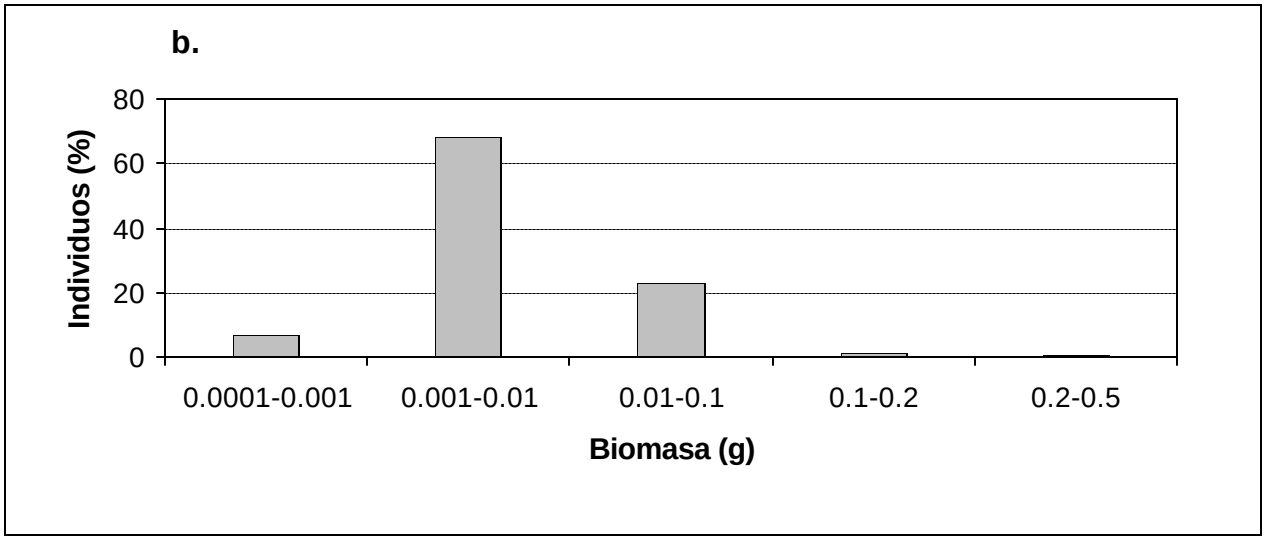

Figura 9. Rangos de Longitud Total -LT- (a.) y Biomasa (b.), de postlarvas y juveniles de camarones *Xiphpenaeus kroyeri.* Boca de la Barra (CGSM), febrero 1998 - febrero 1999.

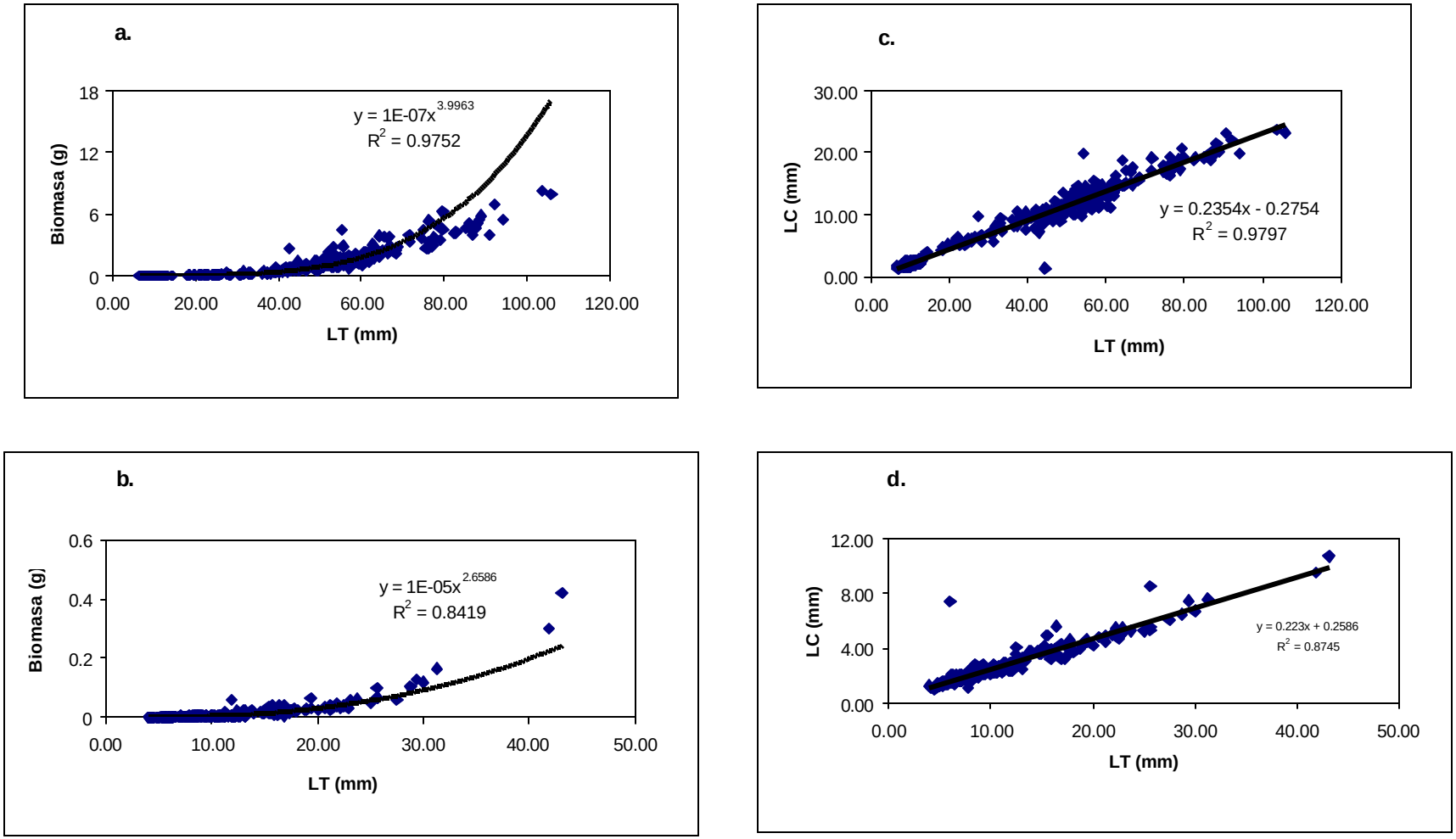

Figura 10. Relaciones Longitud Total (LT) - Peso (a. *Farfantepenaeus spp.* y b. *Xiphopenaeus kroyeri*) y Longitud Total (LT) - Longitud Caparazón (LC) (c. *Farfantepenaeus spp.* y d. *X. kroyeri*) . Boca de la Barra (CGSM), febrero 1998 - febrero 1999.